FOXC1 is required for normal cerebellar development and is a major contributor to chromosome 6p25.3 Dandy-Walker malformation

Kimberly A. Aldinger[1], Ordan J. Lehmann[4], Louanne Hudgins[5], Victor V. Chizhikov[2], Alexander G. Bassuk[6], Lesley C. Ades[7], Ian D. Krantz[8], William B. Dobyns[2,3], and Kathleen J. Millen[1-3]

[1]Committee on Neurobiology, [2]Departments of Human Genetics and [3]Neurology, The University of Chicago, Chicago, Illinois, USA; [4]Departments of Ophthalmology and Medical Genetics, University of Alberta, Edmonton, Canada; [5]Division of Medical Genetics, Department of Pediatrics, Stanford University, Stanford, California, USA [6]Department of Pediatrics, Division of Neurology and the Interdisciplinary Graduate Program in Genetics, University of Iowa, Iowa City, Iowa, USA; [7]Department of Clinical Genetics, The Children's Hospital at Westmead and Discipline of Paediatrics and Child Health, University of Sydney, New South Wales, Australia; [8]Division of Human Genetics, The Children's Hospital of Philadelphia, Philadelphia, Pennsylvania, USA

Supplementary Note regarding the main text

Penetrance, expressivity and modifying factors

Among our patient cohort the brain phenotypes are highly penetrant but exhibit variable expressivity, recapitulating perfectly the ocular phenotypes attributable to *FOXC1*-associated disease[1]. The sole example of apparent non-penetrance is the patient with ring chromosome 6, who has a more extensive genomic alteration deleting part of 6q27[2] and limiting comparisons with other subjects (n = 20). Interestingly, this individual, despite having normal vermis size, does exhibit some posterior fossa pathology comprising a meningeal defect with gyral herniation through the tentorial notch (**arrow in Fig. 2h**). Our results resemble *PAX6*-associated eye and brain phenotypes, which are also highly penetrant and exhibit variable expressivity [3,4].

Our data also shows a similar brain phenotype in patients with deletions and duplications encompassing *FOXC1*, again recapitulating the ocular phenotypes. The mechanisms by which increased or decreased *FOXC1* dosage cause comparable phenotypes are unknown. However, the effects of *FOXC1* are mediated through many downstream genes including both heat shock

Nature Genetics: doi:10.1038/ng.422

proteins and *FOXO1A*, a key cell cycle regulator[5]. FOXO1A influences cellular homeostasis when positively or negatively regulated[6], providing one possible explanation for how seemingly similar human disorders could arise from both increases and decreases in *FOXC1* gene dose.

Malformation of cortical development

Analysis of the cerebral cortex in the mouse *Foxc1*$^{hith/hith}$ hypomorph showed defects in the basement membrane allowing inappropriate migration of neurons into the subarachnoid space and onto the surface of the brain [7]. This was reported to resemble the cobblestone cortical malformation seen in dystroglycanopathies in both mouse and humans, which include Fukuyama congenital muscular dystrophy, muscle-eye-brain disease, and Walker-Warburg syndrome [8-17]. A cobblestone-like cortical malformation has been demonstrated in mice [18] and in humans with homozygous mutations of *GPR56* (**Supplementary Figure 6b**). None of the brain-imaging studies in our 6p25.3 CNV or *FOXC1* mutation patients demonstrated a cortical malformation (**Supplementary Figure 6c-h**). Thus, mutation of *FOXC1* in humans does not cause a visible cortical malformation and is not in any way comparable to the severe cortical malformation found in patients with mutations of *GPR56* or with any of the dystroglycanopathies.

Malformations of meningeal development

Because our analysis of *Foxc1* expression implicated cranial mesenchyme, we specifically examined brain-imaging studies from our 6p25.3-*FOXC1* subjects for defects in the meninges, which are derived from cranial mesenchyme and neural crest. We found two distinct types of meningeal defects consisting of (1) interdigitation of right-left gyri across the midline as shown in **Supplementary Figure 6c-d** and (2) herniation of mesial posterior gyri through an enlarged tentorial notch into the posterior fossa as seen in **Figure 2d-h-j**. Overall, we observed one or both types of meningeal defects in 6/17 patients in this study. We also found enlarged posterior fossa size in 12/21 patients.

Intracranial malformations related to defective development of the meninges have not been widely recognized, but have been reported. In our much larger (n = 5,300 as of early 2009) cohort of patients with brain malformations and related developmental disorders, we have observed similar meningeal abnormalities. For example, we have observed interdigitation of right-left gyri across the midline in several patients with total or severe partial agenesis of the corpus callosum (ACC), most often in the mesial frontal region just anterior to the genu of the corpus callosum. This implies deficiency of the falx cerebri in this region. We have observed

Nature Genetics: doi:10.1038/ng.422

herniation of mesial posterior gyri into the posterior fossa in several patients with cerebellar hypoplasia who do not have deletion 6p25.3. This malformation has been reported in patients with enlarged parietal foramina or “Catlin marks” including several with mutations of *ALX4*, which is expressed in cranial mesenchyme and the developing skull[19-22].

These data lead us to hypothesize that developmental disorders of the mesenchyme may contribute to other forms of MCM and DWM, as well as to other brain malformations beyond MCM and DWM. We recommend that the presence or absence of these meningeal defects become part of the standard evaluation of brain imaging studies, certainly among individuals with developmental disorders.

White matter abnormalities

Several of our 6p25.3 CNV and *FOXC1* mutation patients had patchy white matter signal abnormalities typical of prominent perivascular or Virchow-Robin spaces (**Supplementary Figure 6e-h**). We did not find any evidence for recent or old strokes.

Nature Genetics: doi:10.1038/ng.422

Supplementary Figures

Supplementary Figure 1

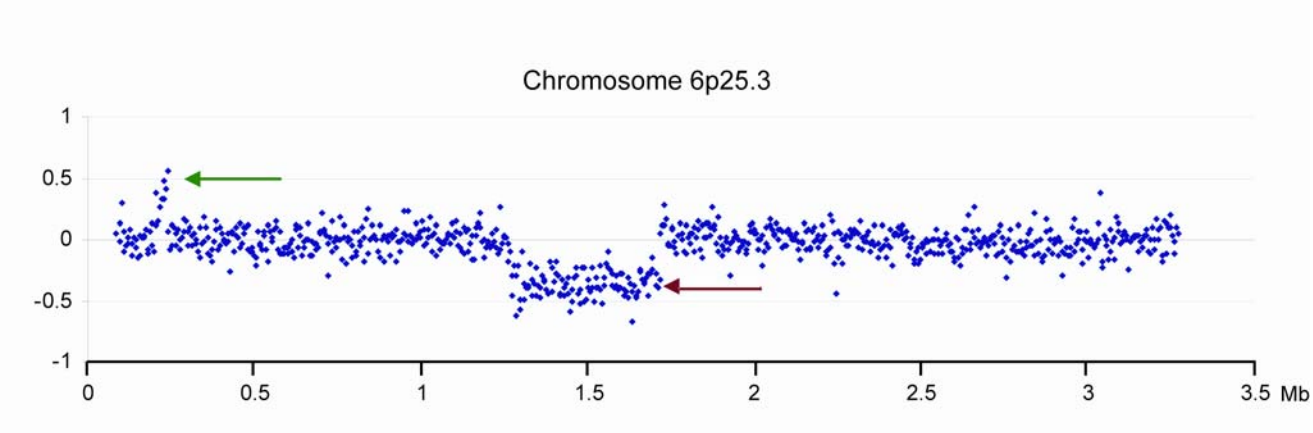

Supplementary Figure 1. Telomeric chromosome 6p aCGH results for patient LR08-198 show the presence of a recognized CNV polymorphism (green arrow) and an abnormal segmental deletion (red arrow). Chromosome position (NCBI Build 35) is shown along the X-axis, log2 Cy3:Cy5 ratio is shown along the Y-axis.

Nature Genetics: doi:10.1038/ng.422

Supplementary Figure 2

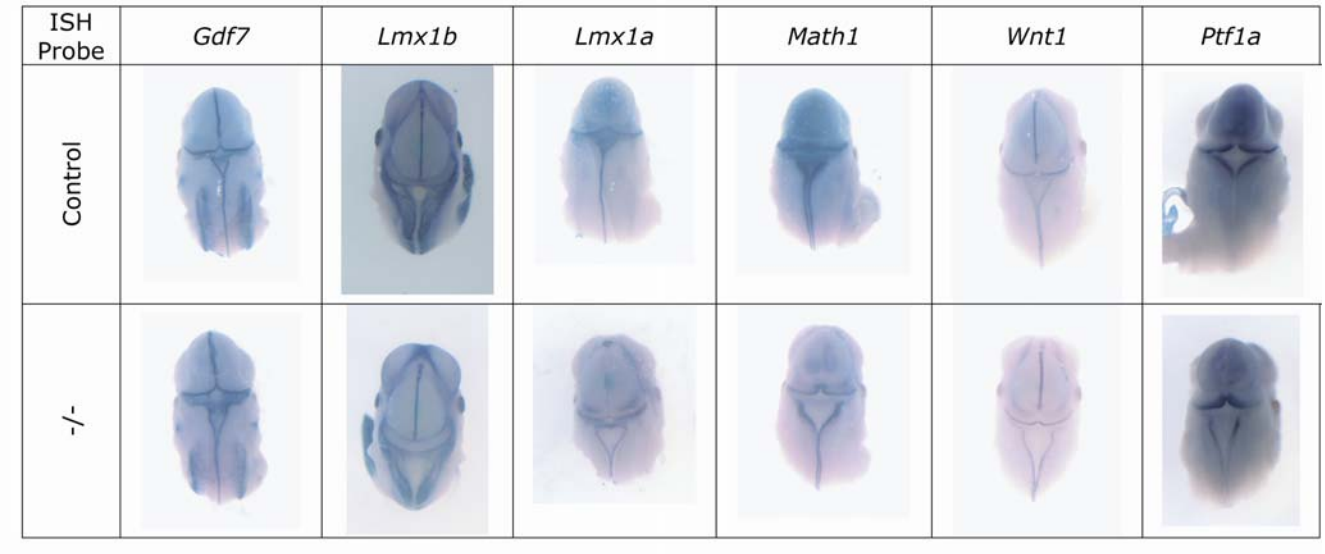

Supplementary Figure 2. Dorsal views of heads showing the expression of six genes important for early roof plate induction, rhombic lip specification and cerebellar anlage patterning in e12.5 WT and *Foxc1*$^{-/-}$ littermate embryos, as assayed by ISH. Markers are indicated. Normal expression for all six genes is observed in the hindbrain of mutant embryos.

Nature Genetics: doi:10.1038/ng.422

Supplementary Figure 3

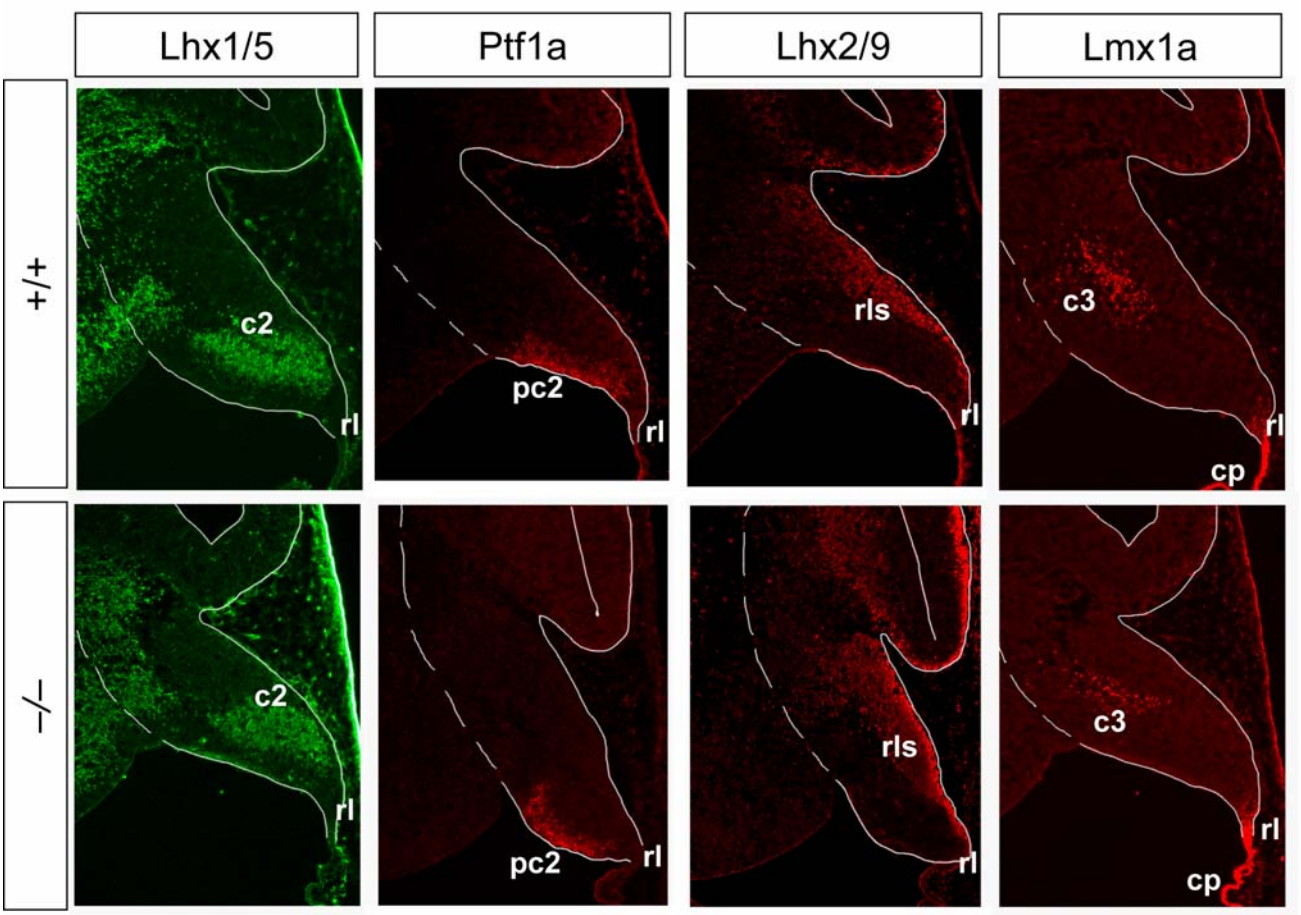

Supplementary Figure 3. Cellular populations within the e12.5 cerebellar anlage. Paramedial sagittal immunostained sections through dorsal rhombomere 1 in WT and *Foxc1*$^{-/-}$ littermate embryos. Markers are indicated. All cellular populations are present in the expected domains of the cerebellar anlage in the mutant embryos. c2 and c4 cells are Lhx1/5+. Ptf1a+ pc2 cells are progenitors of the Lhx1/5+ c2 cells. Lhx2/9+ cells are the first cells to leave the rhombic lip (rl) and migrate through the rostral migratory stream (rls). Lmx1a marks the rl, choroid plexus and c3 cells that are of unknown fate.

Nature Genetics: doi:10.1038/ng.422

Supplementary Figure 4

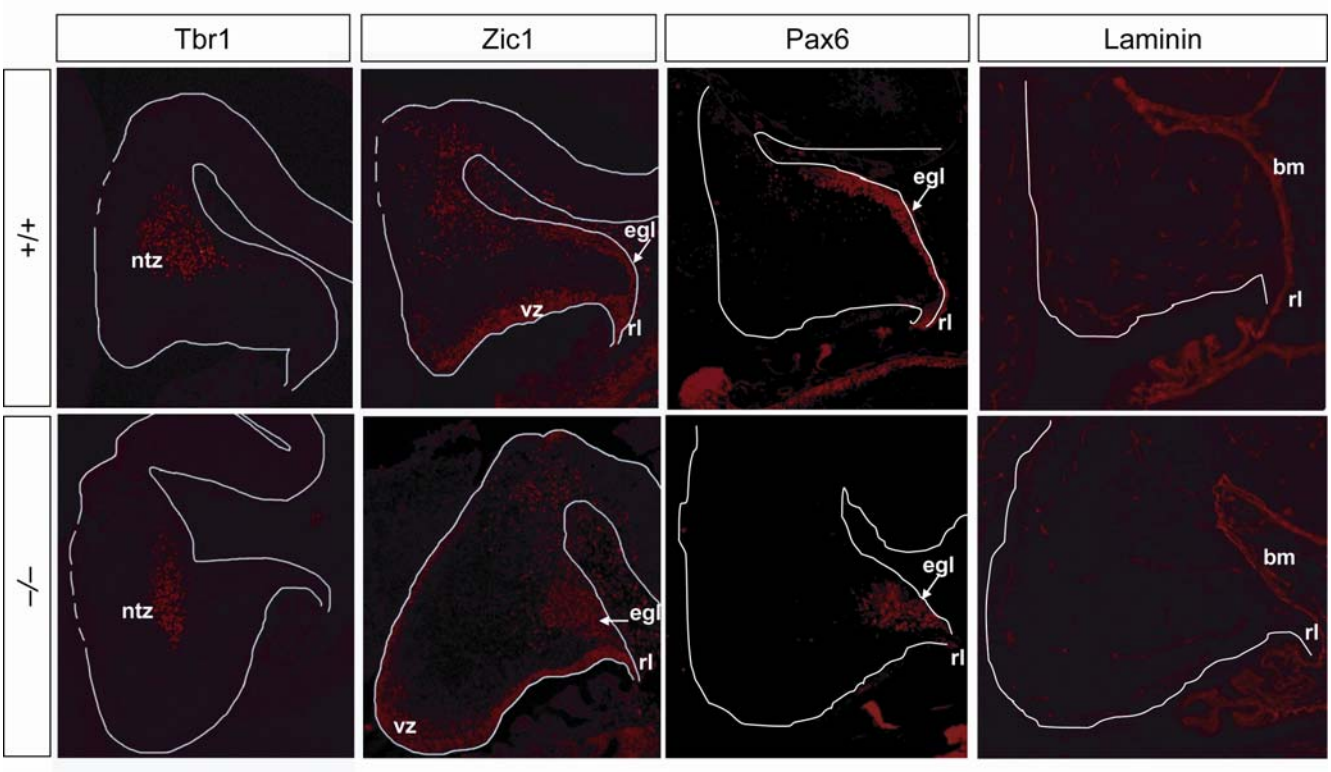

Supplementary Figure 4. Cellular populations within the e14.5 cerebellar anlage. Paramedial sagittal immunostained sections through dorsal rhombomere 1 in WT and *Foxc1*$^{-/-}$ littermate embryos. Markers are indicated. All cellular populations are present in the expected domains of the cerebellar anlage in the mutant embryos. Tbr1+ expression in rhombic lip (lp) derived cells within the nuclear transitory zone (ntz) is present in *Foxc1*$^{-/-}$ embryos. Zic1 and Pax6 label cells within the external granule cell layer (egl). Zic1+ cells also occupy the ventricular zone (vz) in WT and *Foxc1*$^{-/-}$ embryos. Pax6 marks Math1-derived cells from the rl, including cells in the egl. Despite the abnormal clump of cells in the egl of *Foxc1*$^{-/-}$ embryos, Zic1/Pax6+ expression demonstrates that these cells maintain egl progenitor identity. No discontinuity in laminin expression within the basement membrane (bm) at the pial surface of the cerebellum is observed in *Foxc1*$^{-/-}$ embryos.

Nature Genetics: doi:10.1038/ng.422

Supplementary Figure 5

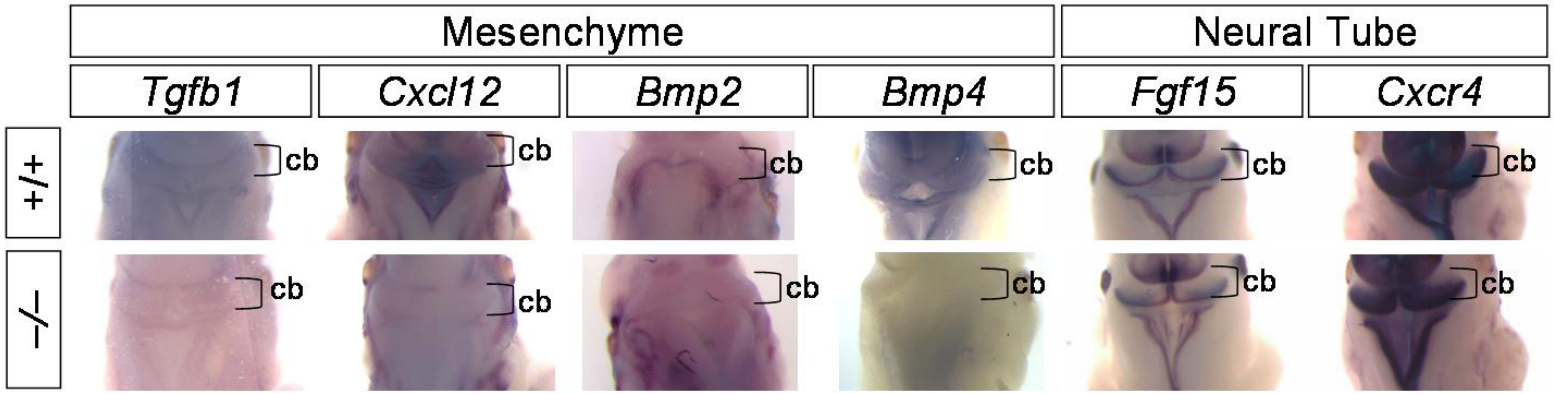

Supplementary Figure 5. Expression of four signaling molecules secreted from mesenchyme and two molecules expressed in hindbrain neural tube in e12.5 WT and *Foxc1*$^{-/-}$ littermate embryos, as assayed by ISH. Dorsal views of heads show all four genes secreted from mesenchyme are down-regulated in the hindbrain of mutant embryos, while the expression of the two genes expressed in the hindbrain neural tube are normal.

Nature Genetics: doi:10.1038/ng.422

Supplementary Figure 6

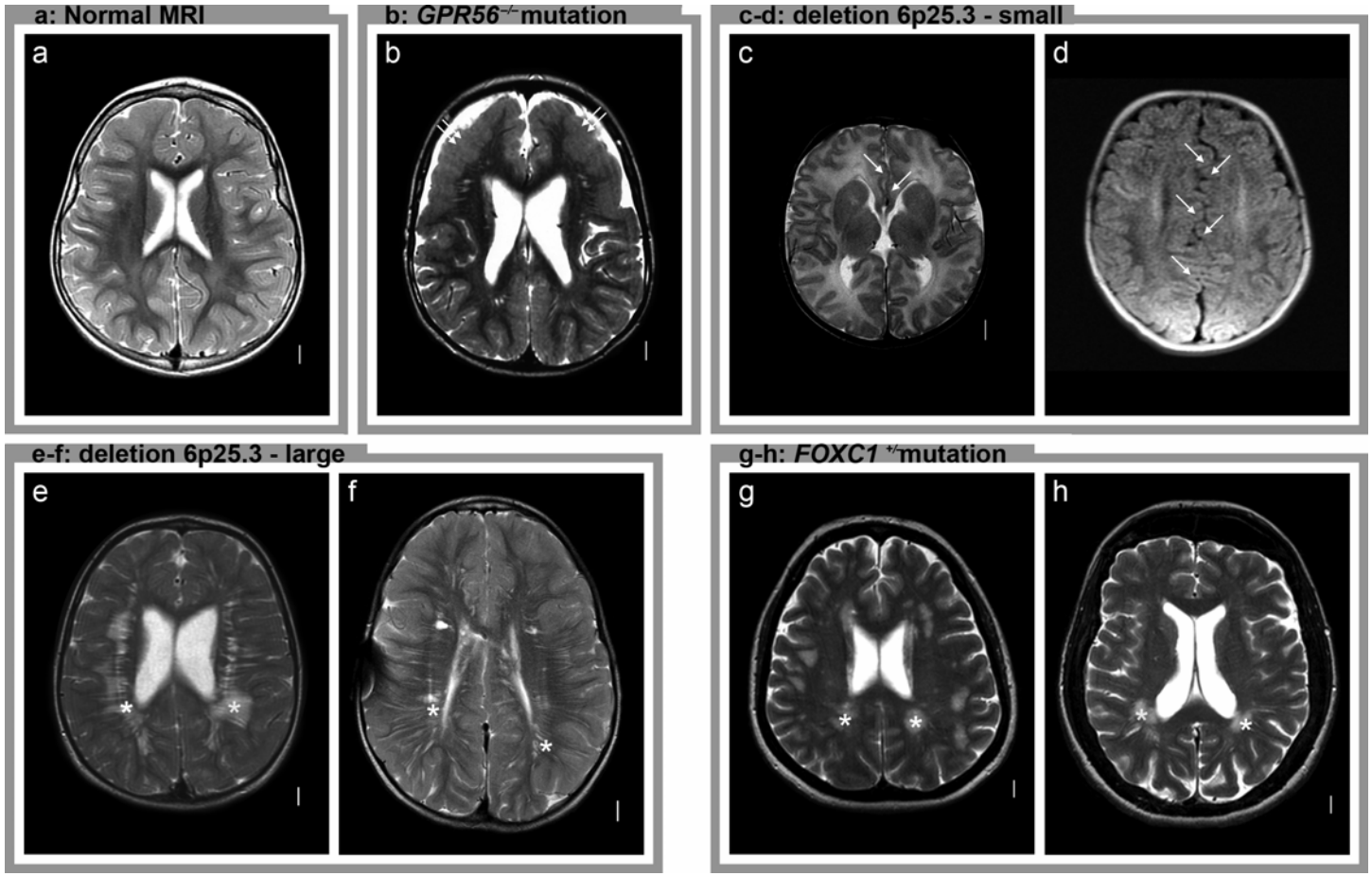

Supplementary Figure 6. T2-weighted (T1- in d) axial magnetic resonance images in a control subject (a), one patient with cobblestone-like cortical malformation associated with homozygous mutation of *GPR56*[23,24] (b), four patients with deletion 6p25.3 (c-f), and two with *FOXC1* mutations (g-h). The scan from the *GPR56*$^{-/-}$ patient shows a thick dysplastic (cobblestone-like) cortical malformation over the frontal lobe that is not seen in any patient with a copy number variant or mutation of *FOXC1*, even though the

Nature Genetics: doi:10.1038/ng.422

Gpr56$^{-/-}$ and *Foxc1*$^{-/-}$ mouse mutants have similar cortical abnormalities. The *GPR56*$^{-/-}$ scan also shows a few areas of abnormal white matter signal. The first two scans from patients with small 6p25.3 deletions show mild (c) or marked (d) abnormal interdigitation of right- and left-sided gyri (arrows) indicating deficiency of the falx. The four scans in the bottom row from patients with deletion 6p25.3 (e-f) or *FOXC1* mutations (g-h) demonstrate white matter changes consistent with prominent perivascular spaces (asterisks in e-h), but we did not find any strokes. These images come from patients LR06-130 (a), LR02-097 (b), LR08-198 (c), LR07-072 (d), LR04-302 (e), LR04-313a2 (f), LR08-027a1 (g) and LR08-075 (h) as listed in **Figure 1**.

Nature Genetics: doi:10.1038/ng.422

Supplementary Figure 7

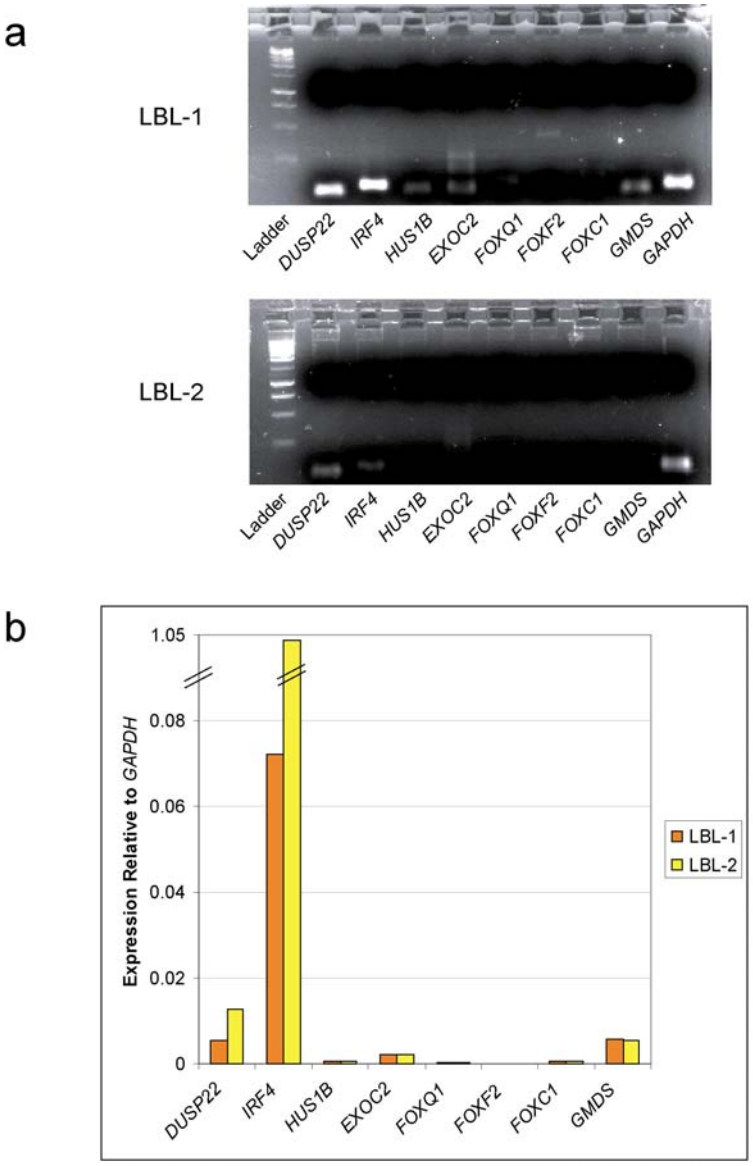

Supplementary Figure 7. Expression of the 6p25.3 DWM locus genes in control lymphoblastoid cell lines (LBLs). (a) Target amplification of 8 genes and *GAPDH* shows that most genes are expressed either at very low or undetectable levels (*FOX* genes) in LBLs from two individuals. (b) qRT-PCR confirms that *IRF4* is the only gene that shows detectable, but variable LBL expression. These results are consistent with publicly available human GeneAtlas (Affymetrix U133A) expression array data (http://biogps.gnf.org/).

Nature Genetics: doi:10.1038/ng.422

Supplementary Tables

Supplementary Table 1. Classical DWM loci identified by cytogenetics.

Locus	N	Mb
del 3q24-q25.1	09	1.9
del 6p25.3	19	1.8
del 13q31.2-q33	07	23
dup 9pter-p11.2	15	47

A comprehensive review of the clinical cytogenetic literature revealed four loci for DWM throughout the genome, each with reports of multiple patients[23-25]. Among patients with DWM and cytogenetic abnormalities encompassing one of the four DWM loci, del 6p25.3 is the most frequent (38%). Among del 6p25.3 patients with MRI or CT images available, we confirmed 33% (19/58) have DWM. del, deletion; dup, duplication; pter, short arm terminus or telomere; N, number of patients; Mb, size of locus in megabases.

Nature Genetics: doi:10.1038/ng.422

Supplementary Table 2. Known gene content of the 6p25.3 DWM critical region.

Known Genes	Mouse developmental expression	Mouse model available	Reported –/– phenotype	–/– Cerebellar phenotype assessment
Dusp22 dual specificity phos	Caudal somites No cerebellum	No	N/A	N/A
Irf4 interferon reg. factor 4	Ubiquitous low level expression throughout embryo including cerebellum	KO[26]	Deficient immune response	Normal
Exoc2 Sec5 exocyst homologue	Ubiquitous throughout embryo, including cerebellum	No	N/A	N/A
Hus1b Hus1 checkpoint homologue	Ubiquitous throughout embryo, including cerebellum	KO (H. Hang unpublished)	N/A	Normal
Foxq1 Forkhead box trans factor q1	Endothelial throughout embryo	*Satin* spontaneous mutant[27]	Coat texture	Normal
Foxf2 Forkhead box trans factor f2	Oral cavity and urogenital system	KO[28]	Cleft palette	Normal
Foxc1 forkhead box trans factorc1	Head mesenchyme including adjacent to hindbrain	*congenital hydrocephalus* spontaneous mutant and KO[29]	Eye, lung, urogenital, skull, heart	Abnormal at e12.5
Gmds GDP-mannose 4, 6-dehydratase	Gastrointestinal No cerebellum	No	N/A	N/A

Nature Genetics: doi:10.1038/ng.422

Supplementary Table 3. Mouse and Human Primer Sequences

Species	Gene	RefSeq	Forward Primer	Reverse Primer	cDNA	gDNA
Mouse	*Bmp2*	NM_007553	GAAGTTCCTCCACGGCTTCT	AGATCTGTACCGCAGGCACT	123	6230
Mouse	*Bmp4*	NM_007554	ATCAAACTAGCATGGCTCGC	TGGACTGTTATTATGCCTTGTTTT	115	1178
Mouse	*Cxcl12*	NM_021704	TTTCAGATGCTTGACGTTGG	GCGCTCTGCATCAGTGAC	102	2867
Mouse	*Cxcr4*	NM_009911	TCCAGACCCCACTTCTTCAG	AGTGACCCTCTGAGGCGTTT	124	2395
Mouse	*Fgf15*	NM_008003	CAGTCCATTTCCTCCCTGAA	TGAAGACGATTGCCATCAAG	124	2553
Mouse	*Foxc1*	NM_008592	CGGCACTCTTAGAGCCAAAT	TTTGAGCTGATGCTGGTGAG	167	167
Mouse	*Gmds*	AK086078	GGAGCAGCCAAACTCTATGC	AAACCAGCCACAAACCTGAC	998	27512
Mouse	*Gapdh*	NM_001001303	TTGATGGCAACAATCTCCAC	CGTCCCGTAGACAAAATGGT	110	1944
Mouse	*Tgfb1*	NM_011577	AAGTTGGCATGGTAGCCCTT	GCCCTGGATACCAACTATTGC	128	6980
Mouse	*Ttr*	NM_013697	GGTGCTGTAGGAGTATGGGC	GGAAGACACTTGGCATTTCC	119	3635
Human	*DUSP22*	NM_020185	GCTGGGATGCACAGGTATTT	GCGGAACAATTGAGCAAGA	98	23249
Human	*EXOC2*	NM_018303	TTTGTGGAGCAAACTGGTGA	AGTCTTCGGCGAGACCTACC	103	55260
Human	*FOXC1*	NM_001453	ACATGTTGTAGGAGTCCGGG	CCTTCTACCGGGACAACAAG	147	147
Human	*FOXF2*	NM_001452	TCCCATTGAAGTTGAGGACG	ACTCGCTGGAGCAGAGCTAC	126	3703
Human	*FOXQ1*	NM_033260	GGATCTTCGCCTTTTTCTCC	CCCATAGTCCACCCAACACT	121	121
Human	*GAPDH*	NM_002046	AATGAAGGGGTCATTGATGG	AAGGTGAAGGTCGGAGTCAA	188	1740
Human	*GMDS*	NM_001500	ATAACGAAGTCCTCCGGCTC	AAATCTGGATGCCAAACGAG	130	187646
Human	*HUS1B*	NM_148659	AGGGCCGTCGTAGGATGTAT	GCCTGAAAACAGAGACCTGG	102	102
Human	*IRF4*	NM_002460	GGGTCTGGAAACTCCTCTCC	CCTGCAAGCTCTTTGACACA	118	3358
Mouse	**Foxc1^{hith}*		CGGCGAGCAGAGCTACTATC	CCTTCACTGCGTCCTTCTTC		484

Amplicon sizes for both complimentary DNA (cDNA) and genomic DNA (gDNA) are listed in basepairs for all RT-PCR primer pairs.
*Primers used to genotype *Foxc1^{hith}* mice.

Nature Genetics: doi:10.1038/ng.422

Supplementary References

1. Alward, W.L. Axenfeld-Rieger syndrome in the age of molecular genetics. *Am J Ophthalmol* **130**, 107-15 (2000).
2. Chanda, B. et al. A novel mechanistic spectrum underlies glaucoma-associated chromosome 6p25 copy number variation. *Hum Mol Genet* **17**, 3446-58 (2008).
3. Hanson, I.M. et al. Mutations at the PAX6 locus are found in heterogeneous anterior segment malformations including Peters' anomaly. *Nat Genet* **6**, 168-73 (1994).
4. Sisodiya, S.M. et al. PAX6 haploinsufficiency causes cerebral malformation and olfactory dysfunction in humans. *Nat Genet* **28**, 214-6 (2001).
5. Berry, F.B. et al. FOXC1 is required for cell viability and resistance to oxidative stress in the eye through the transcriptional regulation of FOXO1A. *Hum Mol Genet* **17**, 490-505 (2008).
6. Burgering, B.M. & Kops, G.J. Cell cycle and death control: long live Forkheads. *Trends Biochem Sci* **27**, 352-60 (2002).
7. Zarbalis, K. et al. Cortical dysplasia and skull defects in mice with a Foxc1 allele reveal the role of meningeal differentiation in regulating cortical development. *Proc Natl Acad Sci U S A* **104**, 14002-7 (2007).
8. Miller, G., Ladda, R.L. & Towfighi, J. Cerebro-ocular dysplasia-muscular dystrophy (Walker-Warburg) syndrome: findings in a 20-week-old fetus. *Acta Neuropathol* **82**, 234-238 (1991).
9. Michele, D.E. & Campbell, K.P. Dystrophin-glycoprotein complex: post-translational processing and dystroglycan function. *J Biol Chem* **278**, 15457-60 (2003).
10. Moore, S.A. et al. Deletion of brain dystroglycan recapitulates aspects of congenital muscular dystrophy. *Nature* **418**, 422-5 (2002).
11. Dobyns, W.B. et al. Diagnostic criteria for Walker-Warburg syndrome. *Am J Med Genet* **32**, 195-210. (1989).
12. Dobyns, W.B., Kirkpatrick, J.B., Hittner, H.M., Roberts, R.M. & Kretzer, F.L. Syndromes with lissencephaly. II: Walker-Warburg and cerebro-oculo-muscular syndromes and a new syndrome with type II lissencephaly. *Am J Med Genet* **22**, 157-195 (1985).
13. Williams, R.S., Swisher, C.N., Jennings, M., Ambler, M. & Caviness V.S., J. Cerebro-ocular dysgenesis (Walker-Warburg syndrome): neuropathologic and etiologic analysis. *Neurology* **34**, 1531-1541 (1984).
14. Haltia, M. et al. Muscle-eye-brain disease: a neuropathological study. *Ann Neurol* **41**, 173-180 (1997).
15. Takeda, S. et al. Fukutin is required for maintenance of muscle integrity, cortical histiogenesis and normal eye development. *Hum Mol Genet* **12**, 1449-59 (2003).
16. Jin, Z. et al. Disease-associated mutations affect GPR56 protein trafficking and cell surface expression. *Hum Mol Genet* **16**, 1972-85 (2007).
17. Piao, X. et al. Genotype-phenotype analysis of human frontoparietal polymicrogyria syndromes. *Ann Neurol* **58**, 680-7 (2005).
18. Li, S. et al. GPR56 regulates pial basement membrane integrity and cortical lamination. *J Neurosci* **28**, 5817-26 (2008).
19. Mavrogiannis, L.A. et al. Haploinsufficiency of the human homeobox gene ALX4 causes skull ossification defects. *Nat Genet* **27**, 17-8 (2001).
20. Reddy, A.T., Hedlund, G.L. & Percy, A.K. Enlarged parietal foramina: association with cerebral venous and cortical anomalies. *Neurology* **54**, 1175-8 (2000).
21. Valente, K.D. & Valente, M. Epilepsy in one family with parietal foramina: an incidental finding? *J Neurol Neurosurg Psychiatry* **75**, 1648-9 (2004).

Nature Genetics: doi:10.1038/ng.422

22. Valente, M., Valente, K.D., Sugayama, S.S. & Kim, C.A. Malformation of cortical and vascular development in one family with parietal foramina determined by an ALX4 homeobox gene mutation. *AJNR Am J Neuroradiol* **25**, 1836-9 (2004).
23. Millen, K.J., Grinberg, I., Blank, M. & Dobyns, W.B. ZIC1, ZIC4 and Dandy-Walker malformation. in *Inborn Errors of Development* (eds. Epstein, C.J., Erickson, R.P. & Wynshaw-Boris, A.) (Oxford University Press, Oxford, 2008).
24. Martinet, D. et al. Subtelomeric 6p deletion: clinical and array-CGH characterization in two patients. *Am J Med Genet A* **146A**, 2094-102 (2008).
25. Ballarati, L. et al. 13q Deletion and central nervous system anomalies: further insights from karyotype-phenotype analyses of 14 patients. *J Med Genet* **44**, e60 (2007).
26. Mittrucker, H.W. et al. Requirement for the transcription factor LSIRF/IRF4 for mature B and T lymphocyte function. *Science* **275**, 540-3 (1997).
27. Hong, H.K. et al. The winged helix/forkhead transcription factor Foxq1 regulates differentiation of hair in satin mice. *Genesis* **29**, 163-71 (2001).
28. Wang, T. et al. Forkhead transcription factor Foxf2 (LUN)-deficient mice exhibit abnormal development of secondary palate. *Dev Biol* **259**, 83-94 (2003).
29. Kume, T. et al. The forkhead/winged helix gene Mf1 is disrupted in the pleiotropic mouse mutation congenital hydrocephalus. *Cell* **93**, 985-96 (1998).

Nature Genetics: doi:10.1038/ng.422